IIETA International Information and Engineering Technology Association
Advancing the World of Information and Engineering

Revue des Composites et des Matériaux Avancés-Journal of Composite and Advanced Materials
Vol. 36, No. 4, August, 2026, pp. 725-732
Journal homepage: http://iieta.org/journals/rcma

Study of the Optical and Electrical Properties of the Co-Sensitization of Red Dragon Fruit and Japanese Papaya Leaves as a Sensitizer of Photoanode

Putu Suardana[1*], Ni Luh Arpiwi[2], Ida Ayu Dwi Giriantari[3], Hery Suyanto[1]

[1] Physics Department, Faculty of Mathematics and Natural Sciences, Udayana University, Badung 80361, Indonesia
[2] Biology Department, Faculty of Mathematics and Natural Sciences, Udayana University, Badung 80361, Indonesia
[3] Department of Electrical Engineering, Faculty of Engineering, Udayana University, Denpasar 80113, Indonesia

Corresponding Author Email: suardanaputu@unud.ac.id

Copyright: ©2026 The authors. This article is published by IIETA and is licensed under the CC BY 4.0 license (http://creativecommons.org/licenses/by/4.0/).

https://doi.org/10.18280/rcma.360404

Received: 12 May 2026
Revised: 14 July 2026
Accepted: 24 July 2026
Available online: 31 August 2026

Keywords:
optical band gap, co-sensitization, Japanese papaya leaf extracts, maceration time, natural dyes, photoanode, red dragon fruit extracts

ABSTRACT

Dyes are an important component of photoanodes. Photoanodes with a single natural dye are limited by wide optical band gaps, narrow-spectrum absorption of visible light, and adverse aggregation of dye molecules. Chlorophyll has strong apparent light absorption, but is susceptible to aggregation at its molecular interfaces. Betacyanin, of small size, is able to break down the aggregation of chlorophyll molecules and enter the gaps between them. Here, it is reported that the co-sensitization strategy uses betacyanin from red dragon fruit (RDF) as a co-sensitizer pair to control the chlorophyll aggregation of Japanese papaya leaf (JPL). Acetone was found to be the most effective solvent for extracting both dyes. The optical and electrochemical properties of co-sensitizers and photoanodes were investigated using ultraviolet-visible (UV-Vis) spectroscopy and cyclic voltammetry. Co-sensitization of RDF dye extract that has been extracted with a maceration time of 6 h (RDFAc6) and JPL extract that has been extracted with a maceration time of 10 h (JPLAc10), with a volumetric ratio of RDFAc6:JPLAc10 of 1:9, was able to produce the lowest indirect optical band gap of 2.59 eV. 14 h of fluorine-doped tin oxide (FTO)/TiO_2 immersion provides the highest occupied molecular orbital to the lowest unoccupied molecular orbital (HOMO-LUMO) level alignment that thermodynamically supports electron injection into the TiO_2 conduction band and dye regeneration. This study revealed that betacyanin effectively suppresses the detrimental aggregation of chlorophyll and expands the area of visible light harvesting, providing a viable strategy in the manufacture of co-sensitizers from RDF and JPL to be used as a sensitizer component of a TiO_2-based photoanode.

1. INTRODUCTION

Devices that utilize photon absorption to drive oxide reactions or supply holes to catalysts require photoanodes. Photoanodes are indispensable in photoelectrochemical water splitting [1] and solar hydrogen production [2], dye-sensitive photoanodes in semi-artificial photosynthesis and dye-sensitized solar cells (DSSCs) [3], and photoelectrochemical CO_2 reduction and solar fuels [4]. Photoanode dyes are molecular or natural chromophores adsorbed on oxide semiconductors to broaden visible-light absorption and enable interfacial charge transfer [5]. The dye molecule regulates light absorption, charge separation, and interfacial charge transfer. Natural dyes are a viable alternative to expensive and scarce ruthenium dyes, due to their low cost, ease of use, abundant availability of resources, and lack of environmental threats [6]. The narrow absorption spectra and wide optical band gap of organic dyes remain major challenges for natural dyes as photoanode sensitizers [7]. Several studies have reported efforts to optimize photoanode function, including cyanoacrylic acid organic dye design for water splitting [1], anchoring natural anthocyanin dye to TiO_2 surfaces to enhance light-harvesting [8], optimizing extraction conditions to maximize the yield and stability of betacyanin from dragon fruit peel for use as a photoanode dye [9], investigating a natural dye from Cnidoscolus aconitifolius anchored to $SrTiO_3$ to improve DSSC performance [10], using natural green and red dyes from Malabar spinach and red spinach as dye co-sensitizers for a TiO_2 photoanode-based DSSC [11], and panchromatic [12] enhancement in solar cell photoelectrodes by co-sensitization of dyenamo red and blue dyes [13].

In this article, it is reported that the co-sensitization strategy was used to obtain a sensitizer with an optical band gap that supports the requirement for the separation of the electrical charge from the highest occupied molecular orbital (HOMO) to the lowest unoccupied molecular orbital (LUMO) and injection into the TiO_2 conduction band. The co-sensitization strategy was carried out through the optimization of the type of solvent, maceration time, variation in the volumetric ratio of the extract, and the soaking time of the fluorine-doped tin oxide (FTO)/TiO_2 substrate in the co-sensitizer dye as independent variables, and the absorption intensity and the

optical band gap of the sensitizer dye extract as dependent variables.

2. MATERIALS AND METHODS

In almost every region in Indonesia, some plants produce dragon fruit at 20–30 tons/ha/year. The largest region planted with and producing dragon fruit is Banyuangi Regency, East Java Province, which is around 6,000 ha. The red dragon fruit (RDF), whose mass is less than 200 g, is mostly unsold; this part is used as a natural dye. Japanese papaya leaf (JPL) is very abundant and has not been widely used either as a vegetable or as a natural dye, offering an abundant and low-cost source of chlorophyll sensitizers; it is very possible to be utilized as a natural dye material for photoanodes. Improving the RDF and JPL extraction process outside of laboratory conditions highlights opportunities and constraints. The availability and standardization of raw material handling allow for reproducibility in larger batches, while continuous extraction systems to resolve optical band gaps, the LUMO levels corresponding to the conduction optical bands of their counterpart semiconductors, and the HOMO levels for their pair's potential redox electrolytes are still challenges at laboratory scale.

The JPL was taken from a garden in Jimbaran, Badung, Bali. RDF and JPL were cleaned with water and then cut into small pieces measuring approximately 2.5 cm × 2.5 cm. The RDF and JPL pieces were dried in a refrigerated chamber at 6–8 ℃ for 21 and 14 days, respectively. Each of these dry pieces was blended (Q2-8050, Multi-function Grinding) and then sifted through an 80-mesh sieve (GB/T6003.1-2022, Shaoxing Shangyu Shengchao Instrument Equipment Co., Ltd). RDF and JPL dry powders were divided into 30 parts, with each part weighing 3 g (using the Analytical scale, Shimadzu AUW220D). The first, second, and third ten parts of RDF dry powder were dissolved in 450 mL of distilled water, 450 mL of acetone, and 450 mL of ethanol, respectively. Each solution was treated with 0.1 mL of 37% hydrochloric acid (HCl) to improve the yield of betacyanin and maintain a bright red hue [14]. Next, each solution was stirred for 4 h with a magnetic stirrer (Thermo Scientific Cimarec SP88857105 Magnetic Stirrer) at 400 rpm at room temperature. In addition, ten solutions for each solvent were macerated for 2, 6, 10, 14, 18, 22, 28, 34, 40, and 48 h, respectively, and stored in the refrigerator at 5 ℃. At the end of the maceration time, all solutions were filtered using Whatman 42 filter paper. All filtrates were evaporated using a Buchi R-300 Rotary evaporator. 0.2 g of each evaporated extract was dissolved in 5 mL of acetone, then 0.1 mL of this solution was diluted with acetone to 2 mL, followed by measurement of its acidity level with an AS218 PH meter before being tested with an ultraviolet-visible (UV-Vis) spectrophotometer. The same procedure was performed for JPL dry powders; however, in this case, in order to improve the extraction yield of chlorophyll-based dyes and inhibit the occurrence of dye degradation, 0.1 mL of 37% HCl was replaced by 0.1 g of sodium bicarbonate ($NaHCO_3$) in each solution [15]. In addition, based on the UV-Vis spectrum of 60 extracts with different solvents and maceration times, each optical band gap was determined using the Tauc Plot method.

The stages of the Tauc plot method [16] are as follows. Based on the data from UV-Vis characterization in the form of wavelength (λ in nm) and absorbance (A). The absorption coefficient (α in cm^{-1}) was calculated using the relationship of $\alpha = 2.303(A/d)$, with d = 1 cm being the cuvette width. The energy of photons ($h\nu$) in electron volts is calculated using the relationship of $h\nu = 1240/\lambda$, with h the Planck constant and ν the photon frequency. Using the Origin 2019b software, columns are created to calculate α, $h\nu$, $(\alpha h\upsilon)^2$, and $(\alpha h\upsilon)^{½}$. Next, a graph is made with $h\nu$ as the x-axis, $(\alpha h\upsilon)^2$ as the y-axis for the direct optical band gap, and $(\alpha h\upsilon)^{1/2}$ as the y-axis for the indirect optical band gap. Using Lambert's equation, i.e. $(\alpha h\nu)^{1/n} = B(h\nu - E_g)$, with B is the Tauc constant, E_g is the optical band gap, and with the value of n = 1/2 and n = 2 are related to the direct and indirect optical band gaps, respectively. The tangent line to the most linear and steepest line on the curve is created and extrapolated. The meeting point of the extrapolated line and the x-axis is the value of the optical band gap of the dye extracts. The same treatment was performed for all the UV-Vis measurement results, resulting in a list of direct and indirect optical band gap values for RDF and JPL extracts.

One dye extract was selected from each RDF and JPL extract to be used as a starting material for the co-sensitizer based on the lowest optical band gap and its absorption intensity in visible light. The co-sensitizer extracts of RDF and JPL were synthesized with a co-sensitizer volume of 10 mL and volumetric ratios of 1:1, 1:4, 1:9, 2:3, 3:2, 3:7, 4:1, 7:3, and 9:1. The optical band gaps were determined based on their UV-Vis spectra using the Tauc Plot method. One of nine variations in the volumetric ratio of the co-sensitizer extracts was selected based on its lowest optical band gap. Selected co-sensitizers from the optimization of the volumetric ratio are adsorbed onto TiO_2 by the immersion method. The FTO/TiO_2 anatase thin film electrode is immersed in a dye co-sensitizer with immersion time variations of 2, 6, 10, 14, 19, and 24 h. The six pieces of FTO/TiO_2 that have been adsorbed by the dye co-sensitizer (FTO/TiO_2/dye co-sensitizer) were then tested with cyclic voltammetry, with FTO/TiO_2/dye co-sensitizer as the working electrode, platinum as the counter electrode, and Ag/AgCl as the reference electrode, to evaluate the suitability of their HOMO-LUMO levels thermodynamically.

3. RESULTS AND DISCUSSION

The pH range of RDF and JPL extracts is 5.0–5.5 and 5.5–6.0, respectively. The UV-Vis spectra of 30 RDF extracts with maceration time variations of 2–48 h are presented in Figures 1(a)-(c) for the RDF extracted with distilled water (RDFDw), with acetone (RDFAc), and with ethanol (RDFEt), respectively. Meanwhile, the UV-Vis spectra for 30 JPL extracts with the same treatment as the 30 RDF extracts are shown in Figures 2(a)-(c), which are marked with JPLDw, JPLAc, and JPLEt, respectively.

3.1 Solvents and light absorption areas

Figure 1 shows the UV-Vis spectrum of RDFDw, RDFAc, and RDFEt. In RDF extraction, acetone shows the strongest absorption compared with distilled water and ethanol. In the UV-Vis spectrum of RDFAc, the main peak is in the near-UV area, which represents the transition of phenolic compounds. The typical betacyanin peak, which usually appears strongly around 535–540 nm, appears here as a broad, low-intensity feature. However, in the context of co-sensitization, molecules

with low absorption often act as highly effective co-adsorbents.

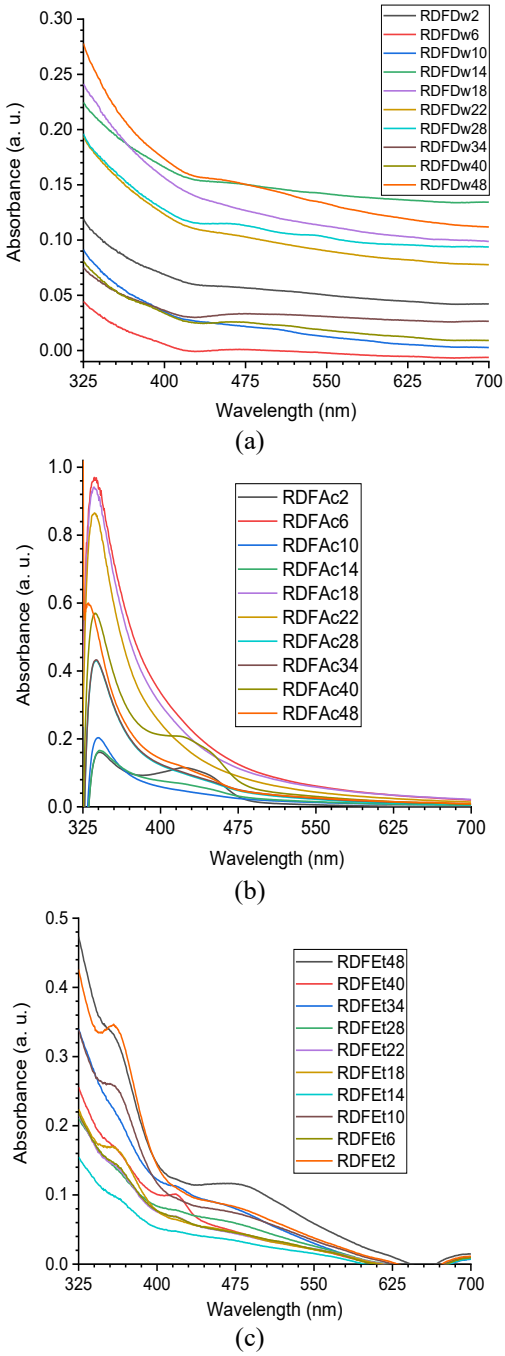

Figure 1. The UV-Vis spectra of RDF: (a) UV-Vis spectra of RDFDw, (b) UV-Vis spectra of RDFAc, and (c) UV-Vis spectra of RDFEt

Note: UV-Vis = Ultraviolet-visible, RDF = red dragon fruit, Dw = distilled water, Ac = acetone, Et = ethanol.

Figure 2 shows the UV-Vis spectra of JPLDw, JPLAc, and JPLEt. In JPL extraction, acetone and ethanol extracted chlorophyll very well, as shown by the high absorption peak intensity. In contrast, distilled water solvents fail to extract these organic pigments. Extracting JPL with ethanol results in absorption peaks in the blue area (430–470 nm) and in the red area (650–670 nm), which are the absorption areas of chlorophyll a and b. In JPLAc, the resulting absorption peaks are almost the same as those of JPLEt. The UV-Vis spectrum of JPLAc has two main absorption bands: the flat, very wide absorption in the blue region (361–435 nm) strongly indicates aggregation of chlorophyll molecules. The absorption shoulder in the 472 nm area is a contribution of carotenoids or is an absorption of chlorophyll b. These pigments help extend light capture beyond chlorophyll a. The absorption bands in the red area have sharp peaks at 665 nm, which are the main characteristics of the low-energy transition of chlorophyll a. In addition, there is also a shoulder absorption at around 606 nm, which supports the presence of chlorophyll. The difference is that the UV-Vis spectrum of JPL extracted with acetone shows absorption peaks at 533 and 560 nm, which are characteristic of betacyanin and are absent in the spectrum of JPLEt. With these more complete absorption peaks, JPLAc (especially for JPLAc10, which has the highest absorption intensity) will complement RDFAc if these two natural dyes are paired as co-sensitizers to expand the area of visible light absorption.

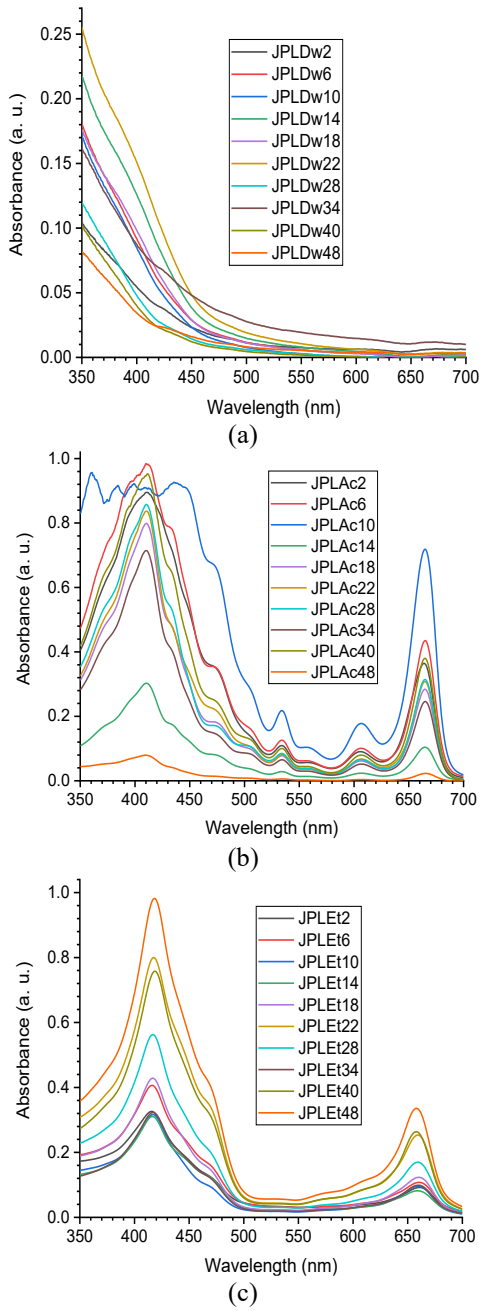

Figure 2. The UV-Vis spectra of JPL: (a) UV-Vis spectra of JPLDw, (b) UV-Vis spectra of JPLAc, and (c) UV-Vis spectra of JPLEt

Note: UV-Vis = Ultraviolet-visible, JPL = Japanese papaya leaf, Dw = distilled water, Ac = acetone, Et = ethanol.

3.2 The dependence of the optical band gaps on the type of solvent used and maceration time

The optical band gap is the minimum energy required by the photoelectron to reach the LUMO level from the HOMO level. A low optical band gap is the initial requirement that a photoanode dye must meet in order to absorb photons in the visible light area. The direct and indirect optical band gaps for RDF and JPL extracts with distilled water, acetone, and ethanol solvents, and with the variation in maceration time of 2–48 h, are shown in Tables 1 and 2, respectively. Figures 3 and 4 show the graphical representation of Table 1, showing the dependence of the direct and indirect optical band gap on solvent type and maceration time of the RDF extracts, respectively. While the graphic form of Table 2 is shown in Figures 5 and 6, for the dependence of the direct and indirect optical band gap on the solvent type and maceration time of the JPL extracts, respectively.

Table 1. The direct and indirect optical band gap of red dragon fruit (RDF) extracts with variations in solvent and maceration time

Maceration Time (h)	RDFDw		RDFAc		RDFEt	
	Direct E_g (eV)	Indirect E_g (eV)	Direct E_g (eV)	Indirect E_g (eV)	Direct E_g (eV)	Indirect E_g (eV)
2	4.04 ± 0.03	3.59 ± 0.02	3.31 ± 0.05	2.67 ± 0.17	4.04 ± 0.20	3.31 ± 0.17
6	4.01 ± 0.01	3.52 ± 0.02	3.31 ± 0.02	2.57 ± 0.11	4.09 ± 0.05	3.59 ± 0.14
10	4.04 ± 0.01	3.62 ± 0.02	3.40 ± 0.01	2.91 ± 0.09	4.06 ± 0.12	3.39 ± 0.19
14	4.01 ± 0.19	3.47 ± 0.02	3.34 ± 0.27	2.65 ± 0.21	4.11 ± 0.06	3.53 ± 0.14
18	4.02 ± 0.16	3.56 ± 0.03	3.36 ± 0.21	2.71 ± 0.19	4.10 ± 0.04	3.53 ± 0.12
22	3.99 ± 0.11	3.45 ± 0.02	3.38 ± 0.13	2.82 ± 0.17	4.09 ± 0.04	3.58 ± 0.13
28	4.04 ± 0.12	3.66 ± 0.02	3.40 ± 0.04	2.87 ± 0.14	4.11 ± 0.02	3.63 ± 0.12
34	3.99 ± 0.01	3.45 ± 0.01	3.39 ± 0.05	2.88 ± 0.13	4.10 ± 0.09	3.61 ± 0.15
40	4.03 ± 0.01	3.57 ± 0.01	3.39 ± 0.17	2.84 ± 0.19	4.09 ± 0.04	3.45 ± 0.13
48	4.02 ± 0.23	3.57 ± 0.03	3.47 ± 0.05	2.98 ± 0.13	3.92 ± 0.12	3.67 ± 0.16

Note: RDFDw = red dragon fruit extracted with distilled water; RDFAc = red dragon fruit extracted with acetone; RDFEt = red dragon fruit extracted with ethanol.

Table 2. The direct and indirect optical band gap of Japanese papaya leaf (JPL) extracts with variations in solvent and maceration time

Maceration Time (h)	JPLDw		JPLAc		JPLEt	
	Direct E_g (eV)	Indirect E_g (eV)	Direct E_g (eV)	Indirect E_g (eV)	Direct E_g (eV)	Indirect E_g (eV)
2	4.63 ± 0.03	2.53 ± 0.12	2.68 ± 0.09	2.29 ± 0.07	2.80 ± 0.03	2.43 ± 0.09
6	4.52 ± 0.08	3.34 ± 0.18	2.78 ± 0.13	2.37 ± 0.08	2.79 ± 0.04	2.42 ± 0.11
10	4.31 ± 0.06	3.18 ± 0.19	2.59 ± 0.04	2.24 ± 0.11	2.79 ± 0.04	2.45 ± 0.12
14	4.77 ± 0.15	2.25 ± 0.21	2.87 ± 0.01	2.62 ± 0.04	2.82 ± 0.02	2.46 ± 0.09
18	4.43 ± 0.09	3.30 ± 0.19	2.86 ± 0.05	2.60 ± 0.07	2.79 ± 0.05	2.43 ± 0.13
22	4.89 ± 0.22	2.61 ± 0.23	2.86 ± 0.05	2.59 ± 0.07	2.77 ± 0.17	2.37 ± 0.17
28	4.86 ± 0.02	3.24 ± 0.13	2.85 ± 0.06	2.57 ± 0.07	2.79 ± 0.08	2.43 ± 0.14
34	4.58 ± 0.08	2.42 ± 0.14	2.87 ± 0.03	2.61 ± 0.07	2.79 ± 0.03	2.44 ± 0.11
40	4.65 ± 0.01	2.24 ± 0.12	2.83 ± 0.08	2.47 ± 0.08	2.78 ± 0.16	2.39 ± 0.17
48	4.39 ± 0.01	2.32 ± 0.09	2.89 ± 0.01	2.63 ± 0.03	2.77 ± 0.26	2.38 ± 0.19

Note: JPLDw = Japanese papaya leaf extracted with distilled water; JPLAc = Japanese papaya leaf extracted with acetone; JPLEt = Japanese papaya leaf extracted with ethanol.

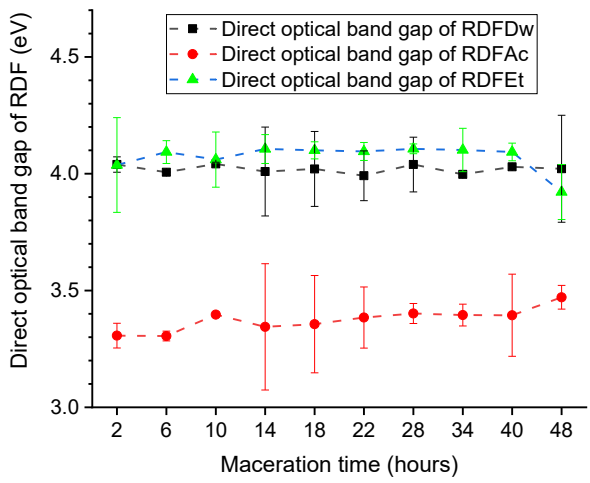

Figure 3. Graph of the dependence of the direct optical band gap on the solvent type and maceration time of the red dragon fruit (RDF) extracts

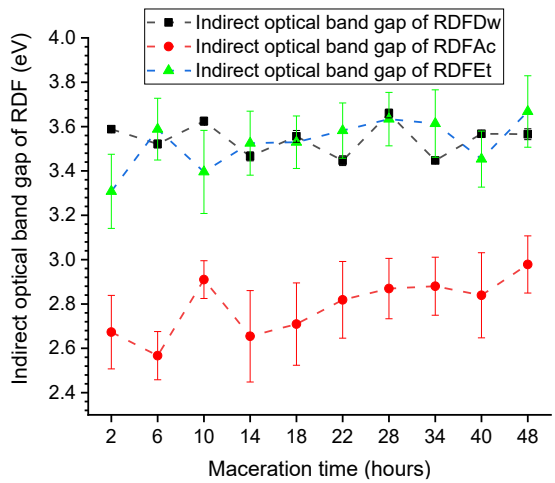

Figure 4. Graph of the dependence of the indirect optical band gap on the solvent type and maceration time of the red dragon fruit (RDF) extracts

RDFAc has smaller and more stable direct and indirect optical band gaps than RDFDw and RDFEt across maceration time. The direct optical band gap of RDFAc is in the range of 3.2–3.4 eV, much smaller compared to the direct optical band gap of RDFDw and RDFEt, which is stable above 4.0 eV. The indirect optical band gap of RDFAc is 2.6–3.0 eV, much smaller than that of RDFDw and RDFEt, which is stable above 3.3 eV. RDFAc6, with an indirect optical band gap of 2.57 ± 0.11 eV, is the smallest optical band gap of all RDFAc, as shown in Figures 3 and 4.

Acetone and ethanol solvents have almost equal power in extracting JPL. Its direct optical band gap is in the range of 2.6–2.9 eV, much smaller than the RDFDw direct optical band gap, which fluctuates at intervals of 4.3–4.9 eV. Meanwhile, its indirect band gap is in the range of 2.2–2.6 eV, much smaller than the highly volatile RDFDw indirect optical band gap, which fluctuates between 2.3–3.3 eV. At the 10-hour maceration time (JPLAc10), the smallest indirect optical band gap was 2.24 ± 0.11 eV, as shown in Figures 5 and 6.

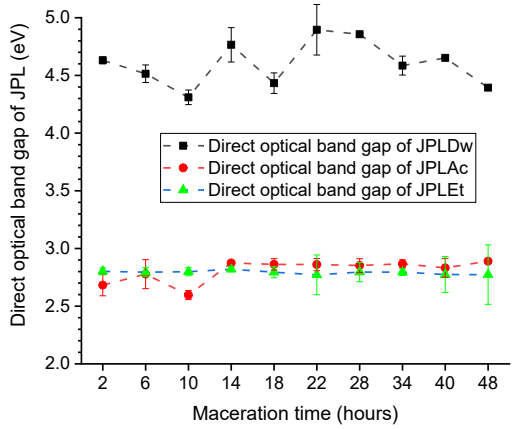

Figure 5. Graph of the dependence of the direct optical band gap on the solvent type and maceration time of the Japanese papaya leaf (JPL) extracts

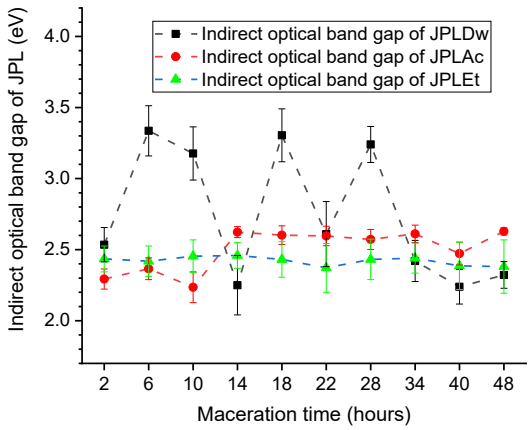

Figure 6. Graph of the dependence of the indirect optical band gap on the solvent type and maceration time of the Japanese papaya leaf (JPL) extracts

Based on the apparent light absorption intensity by RDFAc is higher than the absorption intensity by RDFDw and RDFEt, and the indirect optical band gap of RDFAc6 is the lowest value, as well as based on the high absorption intensity by JPLAc10 in red and blue areas, and there is also a moderate absorption intensity in green-yellow area, and the optical band gap of JPLAc10 extract is also the lowest, therefore, in this initial screening, RDFAc6 and JPLAc10 were selected as the starting materials in the manufacture of the co-sensitizer that will be used as sensitizers for photoanodes.

3.3 The volumetric ratio and the optical band gap of the co-sensitizer

In order to obtain a sensitizer capable of absorbing a wide range of visible light, with a narrow optical band gap, and meeting the requirements of electron injection from the LUMO level to the TiO_2 conduction band and electron regeneration at the HOMO level, the two natural dye extracts RDFAc6 and JPLAc10 are co-sensitized together through optimization of the volumetric ratio, with the volume of the co-sensitizer remaining constant.

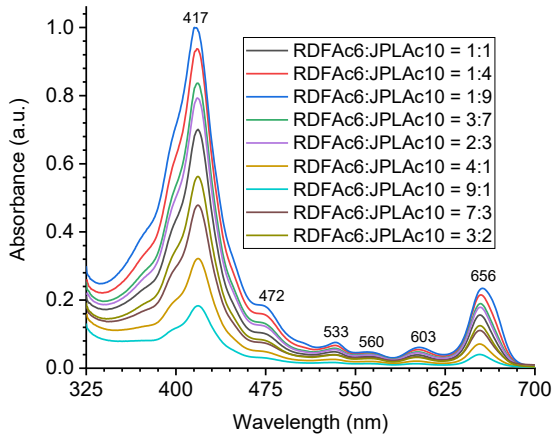

Figure 7. The UV-Vis spectra of RDFAc6 and JPLAc10 extracts as co-sensitizers
Note: Ultraviolet-visible (UV-Vis), red dragon fruit (RDF).

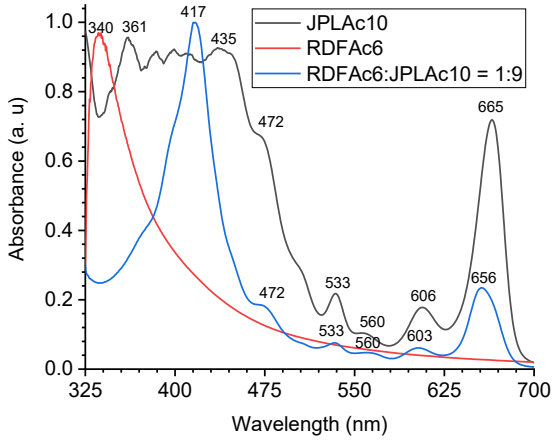

Figure 8. The UV-Vis spectra of RDFAc6, JPLAc10, and co-sensitizer RDFAc6/JPLAc10-1:9
Note: Ultraviolet-visible (UV-Vis), red dragon fruit (RDF), Japanese papaya leaf (JPL).

The RDFAc6 and the JPLAc10 have been mixed as co-sensitizers with a volume of 10 mL and volumetric ratios of 1:1, 1:4, 1:9, 2:3, 3:2, 3:7, 4:1, 7:3, and 9:1. The UV-Vis spectra of these nine co-sensitizers are presented in Figure 7. The spectra of all volumetric ratios show the same absorption peak positions at 417, 472, 533, 560, 603, and 656 nm, but with different absorption intensities. The highest absorption intensity occurs at a volumetric ratio of 1:9. This variation in

the volumetric ratio of co-sensitization suggests that the relative intensity between the peaks of chlorophyll (417 nm and 656 nm) and the peak of betacyanin (533 nm) can be adjusted. The combination of chlorophyll and the conjugated double-bond system of betacyanin shows that this co-sensitization creates a much fuller spectrum of apparent light absorption than using either extract alone.

Figure 8 shows the UV-Vis spectra of RDFAc6, JPLAc10, and the co-sensitization of these two natural dyes with a volumetric ratio of 1:9 (RDFAc6/JPLAc10-1:9). These spectra are taken from Figures 1 and 7, respectively. The interaction between RDFAc6 and JPLAc10 dye molecules in co-sensitization at a volumetric ratio of 1:9 causes the JPLAc10 aggregate to split in the absorption region of 361–435 nm, with RDFAc6 inserting between them as single molecules. This increases the absorption intensity, which becomes very sharp at 417 nm and exceeds the absorption intensity in the UV-Vis spectrum of the JPLAc10 extract (hyperchromic effect) [17-19]. This indicates an increased probability of electron transition at this energy level. In contrast, in the interval from 435 nm to 700 nm, the overall absorption intensity of the co-sensitizer is below the absorption intensity in the UV-Vis spectrum of JPLAc10 (hypochromic effect) [17, 18, 20]. This occurs because the absolute concentration of JPLAc10 in the cuvette is reduced by dilution with 1 part of the RDFAc10, which has low absorption. In co-sensitization, this also causes a counter-buildup of dye molecules, which leads to a breakdown of the excitation energy level that only allows the optical transition to a higher energy level, as shown by the shift of the absorption peak at 606 nm and 665 nm in the JPLAc10 spectrum to the absorption peak at 603 nm and 656 nm in the co-sensitizer spectrum (hypsochromic effect) [16, 17].

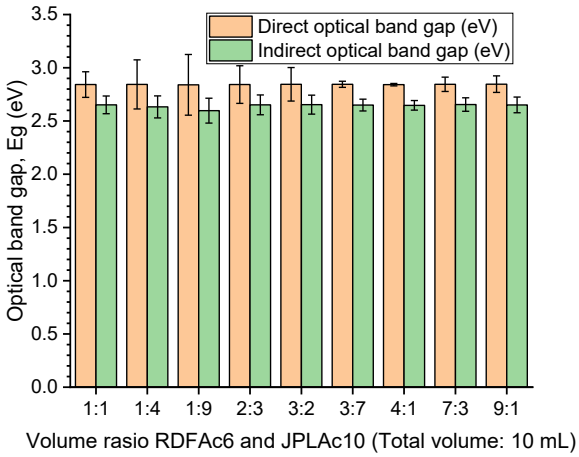

Figure 9. Direct and indirect optical band gaps of co-sensitizers with variation of volumetric ratio of RDFAc6:JPLAc10
Note: Red dragon fruit (RDF), Japanese papaya leaf (JPL).

In a co-sensitization system, the volumetric ratio between two single dye extracts affects the optical band gap generated by the co-sensitizer. In this study, we generated the minimum optical band gap by optimizing the volumetric ratio of RDFAc6 and JPLAc10 dyes with the co-sensitizer volume kept constant. The direct and indirect optical band gaps of the nine co-sensitizer dyes from RDFAc6 and JPLAc10 were determined by the Tauc Plot method; the results are shown in Figure 9. The indirect optical band gap is lower than the direct optical band gap in all volumetric ratios. The 1:9 volumetric ratio of RDFAc6 and JPLAc10 extracts yielded the lowest optical band gap of 2.59 eV.

Although this co-sensitization shows a hypochromic effect due to dilution and a hypsochromic effect due to the accumulation of JPLAc10 dye molecules, 10% RDFAc6 dye molecules can cause a hyperchromic effect that sharply increases absorption intensity in the blue region. In addition, this 1:9 volumetric ratio produces the smallest optical band gap, which is expected to support electron dynamics from the HOMO level until they are injected into the TiO_2 conduction band and regenerate electrons at the HOMO level [6].

Thermodynamically, immersion time determines interface properties and the adsorption-desorption balance of dye molecules, which affect the alignment profile of the HOMO-LUMO levels and the TiO_2 conduction band in the photoanode. Therefore, this study optimized the immersion time of FTO/TiO_2 substrates in co-sensitizer dye extracts (RDFAc6/JPLAc10-1:9). Optimization was carried out with variations in immersion time of 2, 6, 10, 14, 19, and 24 h.

Cyclic voltammetry was performed on the six FTO/TiO_2 samples soaked in the co-sensitizer for different immersion times using a three-electrode system with FTO/TiO_2/co-sensitizer dye as the working electrode, platinum as the counter electrode, and Ag/AgCl (3 M KCl) as the reference electrode. The HOMO energy level was estimated from the oxidation onset potential (E_{ox}^{onset}) and converted to the absolute vacuum scale using Eq. (1). The LUMO level was then calculated by Eq. (2), where the optical band gap E_g was obtained from the Tauc plot.

$$E_{HOMO} = -(E_{ox}^{onset} \text{vs. Ag/AgCl} + 4.64)\ \text{eV} \quad (1)$$

$$E_{LUMO} = (E_{HOMO} + E_g)\ \text{eV} \quad (2)$$

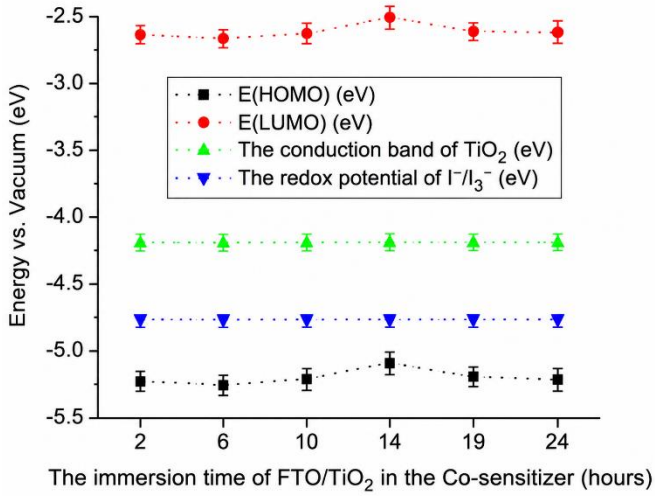

Figure 10. Energy level diagram of the co-sensitizer of RDFAc6/JPLAc10-1:9 adsorbed on FTO/TiO_2 as a function of immersion time
Note: Red dragon fruit (RDF), Japanese papaya leaf (JPL), fluorine-doped tin oxide (FTO).

Figure 10 shows an energy-level diagram of the co-sensitizer RDFAc6/JPLAc10-1:9 adsorbed on FTO/TiO_2 as a function of immersion time. The positions of the TiO_2 conduction band (-4.2 eV) and I^-/I_3^- redox potential (-4.8 eV) are included for reference. The relative positions confirm that the LUMO lies above the conduction band (E_{CB}) of TiO_2, with

a range of driving forces for injection of 1.5–1.7 eV, and the HOMO lies below the redox potential, with a range of driving forces for regeneration of 0.3–0.5 eV, satisfying the thermodynamic requirements for electron injection and dye regeneration.

The immersion time-dependent energy level revealed that the 14-hour immersion time produced the most favorable alignment, with HOMO at -5.11 eV and LUMO at -2.51 eV. This provides the largest driving force for electron injection ($\Delta E_{inj} = E_{LUMO} - E_{CB}\mathrm{Tio}_2 \approx 1.7$ eV), and requires the least reduction potential for dye regeneration ($\Delta E_{reg} = E_{redox} - E_{HOMO} \approx 0.3$ eV). Prolonged immersion beyond 14 h shifts the HOMO level downward to -5.21 eV, which may be attributed to H-aggregation that stabilizes the ground state and reduces the regeneration driving force. This corresponds to hypsochromic shifts from 665 nm to 656 nm and from 606 nm to 603 nm, shown in Figure 8 [21]. Thus, the RDFAc6/JPLAc10-1:9 co-sensitizer, after 14 h of FTO/TiO_2 immersion, is suitable for use as a sensitizer in a TiO_2-based photoanode.

4. CONCLUSIONS

The co-sensitization strategy with a volumetric ratio of 1:9 of RDF and JPL dyes extracted with acetone solvents and maceration times of 6 and 10 h successfully optimized the optical and electronic properties of TiO_2-based photoanodes. Co-sensitization with these two natural dye extracts resulted in the lowest indirect optical band gap of 2.59 eV. Cyclic voltammetry analysis of FTO/TiO_2 immersed for 14 h in the co-sensitizer confirmed the optimal thermodynamic suitability of the HOMO-LUMO level, which strongly supports electron injection into the TiO_2 conduction band and efficient dye regeneration. This co-sensitization approach offers a potential strategy to suppress adverse chlorophyll aggregation, and long-term stability studies are needed to validate its application.

ACKNOWLEDGMENT

Many thanks are extended to the Research, Education and Community Service of Udayana University for the support of this research with research contract No: B/325.1/UN14.4.A/PT.01.03/2026, as well as the head and staff of the Integrated Laboratory, Faculty of Mathematics and Natural Sciences, Udayana University, for the support of its facilities.

REFERENCES

[1] Ansón-Casaos, A., Benito, A.M., Maser, W.K., Orduna, J., Villacampa, B., Blesa, M.J. (2025). Hybrids of deep HOMO organic cyanoacrylic acid dyes and graphene nanomaterials for water splitting photoanodes. Materials, 18(2): 463. https://doi.org/10.3390/ma18020463

[2] Akhmetzhanov, N., Zhang, M., Lee, D., Hwang, Y.H. (2024). PCDA/ZnO organic–inorganic hybrid photoanode for efficient photoelectrochemical solar water splitting. Materials, 17(17): 4259. https://doi.org/10.3390/ma17174259

[3] Prakash, P., Janarthanan, B. (2023). Review on the progress of light harvesting natural pigments as DSSC sensitizers with high potency. Inorganic Chemistry Communications, 152: 110638. https://doi.org/10.1016/j.inoche.2023.110638

[4] Tam, B., Pike, S.D., Nelson, J., Kafizas, A. (2025). The scalable growth of high-performance nanostructured heterojunction photoanodes for applications in tandem photoelectrochemical-photovoltaic solar water splitting devices. Chemical Science, 16(18): 7794-7810. https://doi.org/10.1039/d4sc08595g

[5] Golshan, M., Osfouri, S., Azin, R., Jalali, T., Moheimani, N.R. (2021). Co-sensitization of natural and low-cost dyes for efficient panchromatic light-harvesting using dye-sensitized solar cells. Journal of Photochemistry and Photobiology A: Chemistry, 417: 113345. https://doi.org/10.1016/j.jphotochem.2021.113345

[6] Rahman, S., Haleem, A., Siddiq, M., et al. (2023). Research on dye sensitized solar cells: Recent advancement toward the various constituents of dye sensitized solar cells for efficiency enhancement and future prospects. RSC Advances, 13(28): 19508-19529. https://doi.org/10.1039/d3ra00903c

[7] Keremane, K.S., Abdellah, I.M., Eletmany, M.R., Naik, P., Anees, P., Adhikari, A.V. (2025). Push-pull carbazole twin dyads as efficient sensitizers/co-sensitizers for DSSC application: Effect of various anchoring groups on photovoltaic performance. Journal of Materials Chemistry C, 13(18): 9258-9275. https://doi.org/10.1039/d4tc04612a

[8] Woldu, A.R., Ayele, D.W., Habtu, N.G., Tsigie, Y.A. (2020). Anthocyanin components for dye-sensitized solar cells extracted from Teclea Shimperi fruit as light-harvesting materials. Materials Science for Energy Technologies, 3: 889-895. https://doi.org/10.1016/j.mset.2020.11.001

[9] Sambasevam, K.P., Yunos, N., Mohd Rashid, H.N., et al. (2020). Evaluation of natural pigment extracted from dragon fruit (Hylocereus Polyrhizus) peels. Scientific Research Journal, 17(2): 33-43. https://doi.org/10.24191/srj.v17i2.8989

[10] Vijendran, V., Balasundharam, J., Dinesh, A., Hashem, M., Fouad, H., Santhamoorthy, M. (2024). Photon sensitizer by amalgamation of $SrTiO_3$ and dyes from Cnidoscolus aconitifolius with different pH values for the extensive sustainability of the dye sensitized solar cell. Optical Materials, 157: 116233. https://doi.org/10.1016/j.optmat.2024.116233

[11] Kabir, F., Bhuiyan, M.M.H., Manir, M.S., Rahaman, M.S., Khan, M.A., Ikegami, T. (2019). Development of dye-sensitized solar cell based on combination of natural dyes extracted from Malabar spinach and red spinach. Results in Physics, 14: 102474. https://doi.org/10.1016/j.rinp.2019.102474

[12] D'Amico, F., de Jong, B., Bartolini, M., et al. (2023). Recent advances in organic dyes for application in dye-sensitized solar cells under indoor lighting conditions. Materials, 16(23): 7338. https://doi.org/10.3390/ma16237338

[13] Hupfer, M., Wahyuono, R.A., Dietzek-Ivanšić, B., Plentz, J. (2025). Co-sensitization of red and blue for dye-sensitized solar cells: A sequential approach. Journal of Chemical Sciences, 137(1): 7. https://doi.org/10.1007/s12039-024-02330-1

[14] Permana, L., Sriprom, P., Manamoongmongkol, K.,

Phumjan, L., Assawasaengrat, P. (2025). Optimization of betalain extraction from dragon fruit (Hylocereus undatus) peel and effect of pH on its properties. Biomass Conversion and Biorefinery, 15(3): 3545-3556. https://doi.org/10.1007/s13399-023-05260-z

[15] Sari, P.D., Wijaya, I.M.A.S., Giriantari, I.A.D., Wartini, N.M., Hartati, R.S. (2025). Chlorophyll and magnesium content of papaya leaves extract (Carica papaya L.) at Various Extraction Times. Journal of Agricultural Sciences – Sri Lanka, 20(1): 110-118. https://doi.org/10.4038/jas.v20i1.10110

[16] Jubu, P.R., Obaseki, O.S., Ajayi, D.I., et al. (2024). Considerations about the determination of optical bandgap from diffuse reflectance spectroscopy using the Tauc plot. Journal of Optics, 53(5): 5054-5064. https://doi.org/10.1007/s12596-024-01741-0

[17] Estiningtyas, I.W., Kusumawati, N., Setiarso, P., et al. (2023). Effect of natural dye combination and pH extraction on the performance of dye-sensitized photovoltaics solar cell. International Journal of Renewable Energy Development, 12(6): 1054-1060. https://doi.org/10.14710/ijred.2023.56172

[18] Amogne, N.Y., Ayele, D.W., Tsigie, Y.A. (2020). Recent advances in anthocyanin dyes extracted from plants for dye sensitized solar cell. Materials for Renewable and Sustainable Energy, 9: 23. https://doi.org/10.1007/s40243-020-00183-5

[19] Maylinda, E.V., Rinadi, A., Putri, E.A., Fadillah, G., Wayuningsih, S. (2019). Color stability of anthocyanins copigmentation from red rice (Oryza sativa L.) Bran by spectrophotometry UV-Vis. IOP Conference Series: Materials Science and Engineering, 578: 012001. https://doi.org/10.1088/1757-899X/578/1/012001

[20] Setiarso, P., Harsono, R.V., Kusumawati, N. (2023). Fabrication of dye sensitized solar cell (DSSC) using combination of dyes extracted from curcuma (Curcuma xanthorrhiza) rhizome and binahong (Anredera cordifolia) leaf with treatment in pH of the extraction. Indonesian Journal of Chemistry, 23(4): 924-936. https://doi.org/10.22146/ijc.77860

[21] Joseph, I., Louis, H., Okon, E.E.D. (2023). Experimental and theoretical study of the dye-sensitized solar cells using Hibiscus sabdariffa plant pigment coupled with polyaniline/graphite counter electrode. Pure and Applied Chemistry, 94(7): 901-912. https://doi.org/10.1515/pac-2022-0103